Biomass Conversion and Biorefinery (2022) 12:1435–1448
https://doi.org/10.1007/s13399-020-00838-3

ORIGINAL ARTICLE

Study on chemical kinetics and characterization of nanosilica from rice husk and rice straw in the fixed-bed pyrolysis process

Neha Gautam[1] · Athira Merlin Rose K. V.[1,2] · Ashish Chaurasia[1]

Received: 30 March 2020 / Revised: 11 June 2020 / Accepted: 19 June 2020 / Published online: 26 June 2020

Abstract

Rice husk (RH) and rice straw (RS) are important by-products from the rice industry. When RH and RS are subjected to pyrolysis, the products include char, tar, and a gaseous mixture containing syngas. In this study, silica was obtained by subjecting char to alkaline extraction. The obtained silica was modified to fit sophisticated industrial applications by adding alcohol and water during extraction in an optimized silicate:alcohol:water ratio. Methanol (MeOH), ethanol (EtOH), and propanol (PrOH) were used as particle size modifiers. The silica obtained were characterized through methods such as Fourier transform infrared spectroscopy (FTIR), X-ray fluorescence (XRF), Brunauer-Emmett-Teller (BET), and field emission scanning electron microscope (FESEM). The obtained silica had an average particle size of 20–170 nm, a high average BET-specific surface area of 328 m^2/g, and a high purity of 98.26%, which enhanced its favorability in the pharmaceutical and food-packaging sectors. FTIR analysis confirmed the presence of Si–O–Si, Si–OH, and Si–O bonds in the silica. A higher purity of silica was obtained from RS than from RH. To obtain high-purity silica, nitrogen should be used as the pyrolyzing agent and acid leaching of the extracted silica should be conducted. To facilitate the design, operation, and economic study of industrial process plant, the clear understanding on kinetics of RH and RS plays a very important role. The kinetic parameters for RH and RS char were estimated through Gaussian distribution of the activation energy model (DAEM).

Keywords Rice husk · Rice straw; p · Pyrolysis · Alkaline extraction · Silica

1 Introduction

Rice is an important cereal crop all over the world. India being a leading rice consumer and producer, the rice cultivating and processing industry has a huge impact on the life of the people. It is estimated that 110.15 million metric tonnes of rice have been produced in the years 2017–2018 [1]. Rice husk and straw are some of the main agricultural by-products resulting from a rice processing industry. For every ton of rice being cultivated or processed approximately, 0.2 ton of rice husk and 1.35 ton of rice straw are brought out as by-products [2]. Other by-products from the rice industry include rice bran. Despite its magnitude being similar to that of rice husk and straw, it is processed and utilized as cattle feed or fertilizer. Being of no nutritional value, rice husk and rice straw cannot be used in the nutritional field. Hence, the problem of waste management arises. Rice straw being generated in magnanimous quantities also needs a proper management system. The importance of the need becomes graver since huge pollution has been created due to the open combustion of the same. The necessity of managing rice by-products in huge amount as well as the idea of extraction of more value-added products from rice leads to research on silica extraction from rice husk and straw. Rice husk contains approximately 21% of rich husk ash (RHA) which contains around 95% of the silica while rice straw contains 12% of rice straw ash (RSA) which contains 72.8% of silica. Silica finds a number of applications like cement industry, rubber industry, glass industry, ceramics industry, biomedical sector, etc. The silica extracted from RS or RH has numerous applications. When silica extracted from

Electronic supplementary material The online version of this article (https://doi.org/10.1007/s13399-020-00838-3) contains supplementary material, which is available to authorized users.

✉ Ashish Chaurasia
aschaurasia@che.vnit.ac.in

[1] Department of Chemical Engineering, Visvesvaraya National Institute of Technology, Nagpur, Maharashtra State 440010, India

[2] Present address: Production Department of the Fluorochemicals Business, SRF Limited, Dahej, Gujarat State 392130, India

rice husk (RH) or rice ash (RS) is modified to have a nanometer size, it can be used in sophisticated industrial applications, such as ceramics [3], corrosion inhibition [4], rubber filler production [5, 6], nanomaterials production [7], ethanol production [8], polymer composite production [9], and photocatalysis [10]. Moreover, research is being conducted on the application of mesoporous nanosilica in the target drug delivery system [11]. Bajpai et al. [12] have reported the use of RHA as a silica source for the synthesis of zeolites. The increase in the specific surface area of silica particles due to particle size reduction favors their applicability as a catalyst for a wide range of reactions.

Extensive research has been conducted on extraction of silica from rice husk. The char obtained from the pyrolysis of RH contains 20% ash [13], which contains the silica to be extracted. Washing the RH char (RHC) with acid before the extraction procedure increases the silica yield and reduces the moisture content [14–18]. Among the acids HCl, HNO_3, and H_2SO_4, HCl enables the maximum yield of silica, with moisture retention of only 4%. However, it also causes a marginal agglomeration of silica particles. During alkaline extraction, the addition of ethanol helps in obtaining spherical and well-dispersed silica particles [19]. An increase in the addition of ethanol reduces the specific surface area of silica. The pH is also an important factor in the gelation of gel from sodium silicate (SS) solution [20, 21]. An increase in the pH from 7 causes the particles to be well dispersed and more spherical and reduces their specific surface area. A pH higher than 7 causes the formation of hard gels due to agglomeration, whereas a pH less than 7 causes the formation of a dilute suspension that takes more than 2 days to age. The addition of water affects particle formation because an increase in the concentration of the SS solution causes agglomeration of particles. A decrease in the SS concentration reduces the particle diameter and consequently increases the specific surface area. The particle diameter of silica is an important parameter in the application of extracted silica. The particle diameter mainly affects the mechanism of polymerization [22]. Among the alcohols used for the better dispersion of particles, MeOH provides the smallest silica particle size, which varies from 5 to 50 nm [23], whereas ethanol provides a minimum silica particle size of only 45 nm. This result can be explained by the difference in nuclei formation between the two alcohols. The particle size of the formed silica is also proportional to the chain length of alcohol used [24]. It is also suggested that the usage of alcohols beyond butanol is unsuitable for obtaining small-sized silica particles [24]. The washing of residue after the separation of the SS solution by filtration with 100 ml of boiling water helps to efficiently remove any SS trapped in the residue and hence improves the yield of extracted silica [3]. Silica has been extracted from RS char (RSC) by using the aforementioned alkaline extraction procedure. The silica extracted from RSC has been compared with the silica extracted from the RHC.

The temperatures at which RH/RS must be pyrolyzed and the temperature at which inert atmosphere must be supplied are important parameters that influence the overall efficiency of utilizing RH/RS. Nitrogen has been found to be a superior agent compared with air, with superior production of syngas [25]. The temperature of pyrolysis suggested by Kate and Chaurasia [26] was 500–700 °C. The purity of the extracted silica increased on heating it at 700 °C for 1 h. Moreover, the specific surface area of silica decreased with increasing the pyrolysis temperature. Krishnarao et al. [27] reported that the presence of potassium led to surface melting at a high temperature of 800 °C. Therefore, the production of high-purity silica from raw RH requires a temperature of less than 600 °C. The amorphous nature of extracted silica will be converted to crystalline at higher temperatures. The effects of calcinations parameters, such as the temperature, time, and heating rate, on the extraction of silica from RH require thorough kinetic investigation [28, 29]. The burning of RH and RS under well-defined condition is the only way to obtain active RH and RS ash with possible application to prepare high-purity amorphous silica. Hence, to reduce the operating cost and protect the environment, an alternative and more-efficient route to prepare silica powders and also utilizing the value of generated syngas and activated carbon would be of considerable commercial interest. Hence, in the present study, this is done conveniently in a new two-stage process. The conventional methods for the treatment of biomass include combustion, gasification, and pyrolysis. The combustion process due to use of excess oxygen produces a large amount of nitrogen oxide emission whereas gasification process which is carried out in limited supply of oxygen produces gas with a low calorific value and also suffers from tar formation. Tar is one of the major concerns in biomass gasification processes which condense in downstream equipment causing failure of the gasification projects [25, 30]. The fast pyrolysis process aimed at optimizing the bio-oil production and its further upgradation to transport fuels as discussed in our previous work [31]. The treatment of biomass in a new two-stage process is based on pyrolysis in the first stage of the reactor while cracking of tar and other pyrolysis products in the downstream second stage of a reactor at elevated temperature. The two-stage process allows clean and economic production of fuel gas with low tar content and high calorific value [25, 30, 32]. The successive stages of development of the two-stage process were given in our previous research work [25, 31–33] and also reported by many authors [30, 34–38]. This study provides the novel results on the valorization of products from RH and RS using the two-stage process that has not been previously described in the literature. The aim of the present study was to produce high-purity-grade silica from the RH and RS and other by-products such as high-quality activated carbon and clean gas with low tar content using a two-stage process that might be suitable for commercial applications.

The wide range of operating conditions was used to study the effects of feedstock, treatment, and extraction process on the yield, purity, and structure of silica produced that have not been described in the previous literature. A kinetic study was carried out to facilitate the design, operation, and economic study of the plant. A techno-economic analysis was presented for the production of commercial-grade purity levels of silica to reveal the financial feasibility of such a plant.

2 Methodology

The pyrolysis of RH and RS was conducted in a two-stage process (Fig. 1). The detailed design of this reactor is available in our previous research [25, 31–33, 39–41]. The pyrolysis reactions were performed under fixed-bed conditions, and 50 g of RH or RS feed was introduced into the chamber after it attained the temperature of pyrolysis. The temperature of pyrolysis was maintained at 600 °C through a proportional-integral derivative (PID) controller. Nitrogen was supplied to ensure an inert atmosphere with a flowrate of 0.5 l/min. Thus, the effect of the agent (N_2 or air) on the purity of extracted silica could be studied. The second chamber was a gasification reactor, which had a constant and continuous flow of air through it. The temperature of gasification was maintained at 875 °C by using a PID controller. The chamber was filled with 150 g of mild steel (MS) turnings, which increased the contact-specific surface area and enhanced the gasification reaction by acting as a catalyst. The MS turnings were replaced with new ones after every four consecutive runs. The holding time of biomass inside the reactor was fixed between 15 and 20 min by moderating the gas flow through it. The carrier gas swept down the gaseous products, which were collected simultaneously in sample bags. The liquid (tar) and solid (char) products of pyrolysis were collected after 3–4 h of cooling the reaction chamber. The char obtained was collected and weighed.

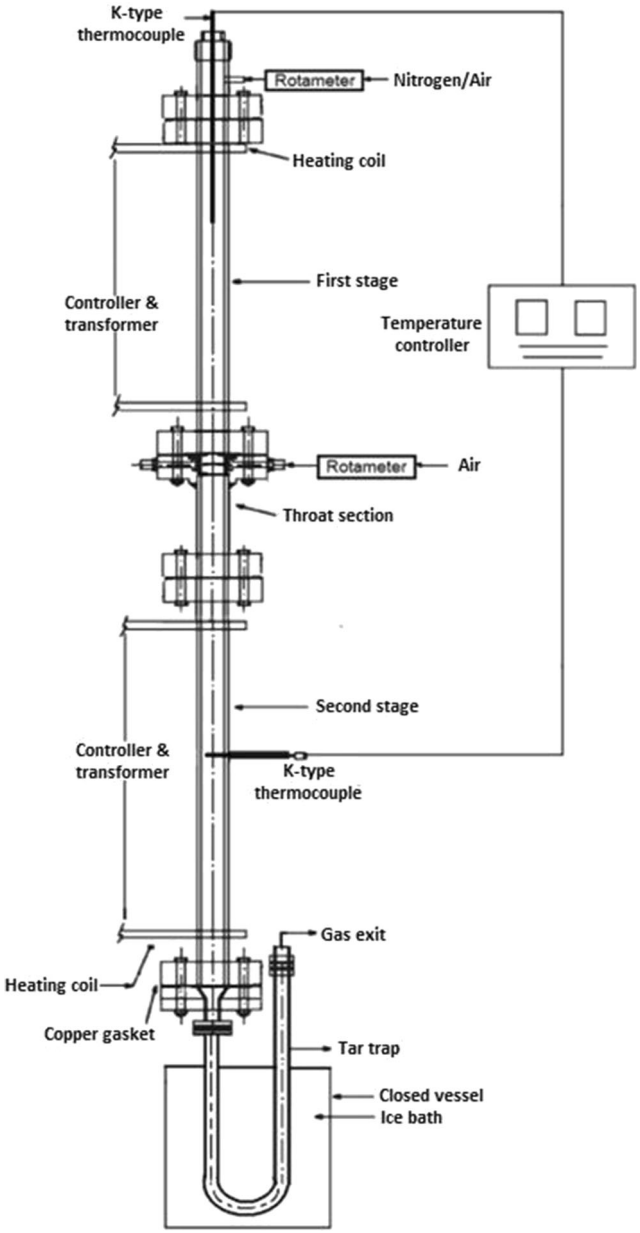

Fig. 1 Schematic of two-stage gasification process

Figure 2 shows the process flow diagram of silica extraction from RH and RS char. The char was added to 200 ml of distilled water and the suspension was made to have a pH of 1 by adding 1 N HCl. The suspension was then stirred for 2 h and filtered. The residue was washed to remove any contaminants. A total of 120 ml of 1 N NaOH was added to the residue, and the solution was heated at 90 °C with continuous stirring for 1 h. The mixture was then cooled and filtered to obtain SS solution. A total of 200 ml of boiling water was used to wash the residue for removing any remaining SS. The SS solution was added with MeOH and water and mixed. As mentioned above, MeOH is used for better dispersion of particles and helps in obtaining spherical and well-dispersed silica particles, which varies from 5 to 50 nm [23]. The addition of water helps to reduce the agglomeration of particles by decreasing the concentration of SS solution. The resulting solution was slowly added with 1 N HCl to gelate silica. The gelated silica was aged for 18 h. The aged gel was then crushed, filtered, and washed several times with distilled water. The sample was then dried in an oven at 110 °C for 18 h. Then, the sample was washed and dried under same conditions again. The silica was crushed to remove lumps and then placed in a muffle furnace at 550 °C for 30 min.

The kinetic study of pyrolysis degraded RH and RS was carried out to estimate the kinetic parameters of RH and RS char. The experimental data were fitted to modified Gaussian distributed activation energy model (DAEM). The experiments were carried out in the two-stage reactor in the temperature range of 450–650 °C at intervals of 50 °C for a reactor length of 60 cm in the nitrogen

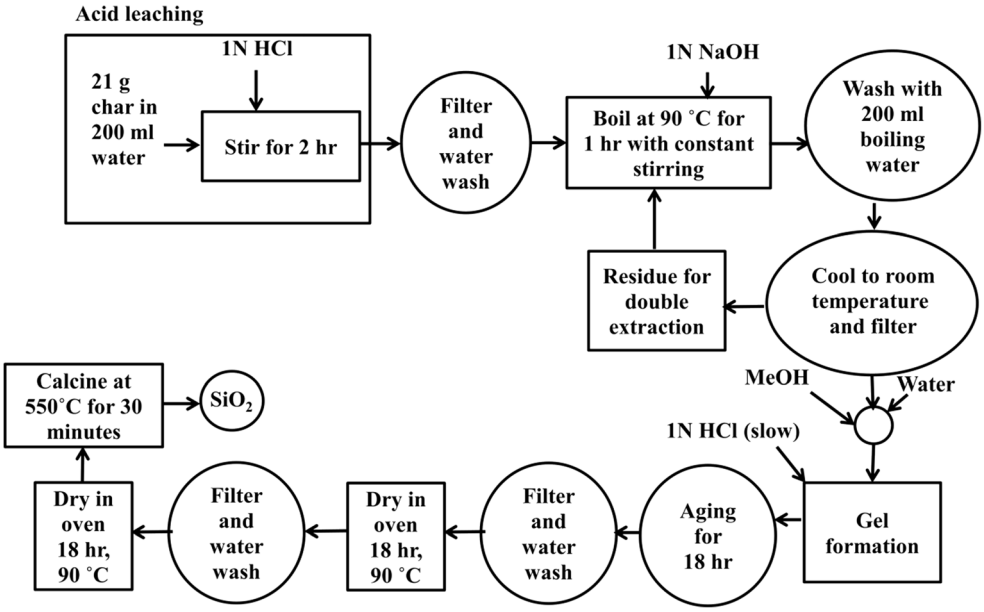

Fig. 2 Process flow diagram of acid leaching and silica extraction from RH and RS char

atmosphere. The char was formed after the complete removal of tar and volatile matters from RH and RS. The nanosilica obtained were also characterized through methods such as FTIR, FESEM, XRF, and BET.

3 Results and discussion

3.1 Kinetic studies

To facilitate the design, operation, and economic study of industrial process plant, the clear understanding on the kinetics of RH and RS plays a very important role. The kinetic parameters A, E, and σ of RH and RS vary which indicate that the design parameters for process plant would be different for the extraction of silica from RH and RS char. As shown in Fig. 3, the weight% of RH char including ash were 45.68, 43.04, 39.26, 37.91, and 37.24% at 450, 500, 550, 600, and 650 °C, respectively, while that of RS char including ash were 37.33, 34.95, 33.93, 32.9, and 32.2% at 450, 500, 550, 600, and 650 °C, respectively. The experimental data on RH and RS char was fitted to modified Gaussian distributed activation energy model given in Eq. (1). This model discussed in detail in our earlier study [31] and found to give better fit as it considers a large number of parallel reactions. The "C" program was written to estimate the kinetic parameters for RH and RS char.

$$V_i = V_i^* \left[\int_0^\infty exp\left(-\int_0^t k_i dt \right) f(E_i)\, dE_i \right] \tag{1}$$

$$f(E_i) = \frac{1}{\sigma_i \sqrt{2\pi}} \exp\left[\frac{-(E-E_{0i})^2}{2\sigma_i^2} \right] \tag{2}$$

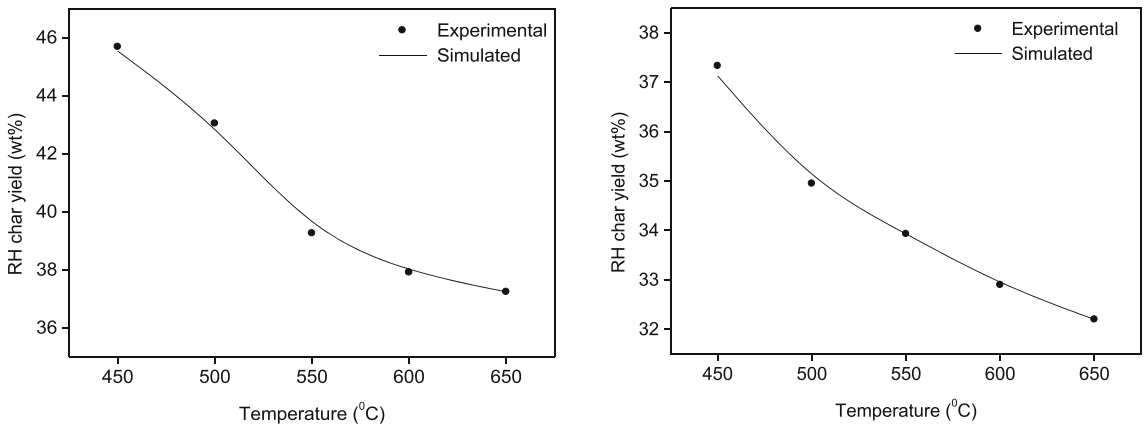

(a) RH Char (b) RS Char

Fig. 3 Yield of **a** RH and **b** RS char against temperature in the result obtained from DAEM simulation

where V_i is the yield of species i at time t; V_i* is the ultimate yield of V_i at the longer residence time and at higher temperature; k_i is the reaction rate equation; and σ_i is the standard deviation of activation energy distribution of species i.

The activation energies were approximated by a continuous distribution function $f(E_i)$ with the activation energies ranging from E_i to $E_i + dE_i$. $f(E_i)dE_i$ denotes the total individual components of the reactions with the mean activation energy E_{0i}. To predict the yield of RH and RS char the integration was conducted over the residence time–temperature history in the reactor over all possible activation energies.

Figure S1a, b shows the standard error in the yield of RH and RS char against the number of iteration in the result obtained from DAEM simulation, respectively. As indicated in the other studies [42–44], the range of frequency factor (A) and activation energy (E) vary widely for RH. Hence, to estimate the best-fit kinetic parameters, the simulation of the present study was carried out for the frequency factor (A) ranging from 10^6 to 10^9 and activation energy (E) ranging from 90 to 150 kJ/mol. It was found from Fig. S1a that the standard error for RH char decreases from 13.7% to less than 0.07% in 21 iterations. The best-kinetic parameters for RH char were $A = 10^{8.7}$ s^{-1}, E = 128.13 kJ/mol, and σ = 5 kJ/mol. As shown in Fig. 3a, the experimental and simulated values of RH char were in very good agreement. The RH char was found to decrease from 45.68% at 450 °C to 37.91% at 650 °C. Figure S1b depicts that the standard error for RS char were decreased from 11.2 to 0.09% in 20 iterations of DAEM model giving the best-fit kinetic parameters for RS char as $A = 10^{8.64}$ s^{-1}, E = 130.33 kJ/mol, and σ = 5 kJ/mol. Figure 3b displays the comparison between the experimental and simulated values of RS char. It was found that the DAEM model had a super fit to the experimental data. The RS char decreases from 37.33% at 450 °C to 32.2% at 650 °C. Table 1 gives the comparison of kinetic parameters of RH and RS char obtained in the present study with three different studies reported in the literature [42–44]. The pre-exponential factor and activation energy of char obtained in the present study matched well with the kinetic parameters of reported studies.

3.2 Effect of methanol addition on yield of silica

Table 2 indicates the effect of different SS:MeOH:H_2O ratios on the silica yield. The process shown in Fig. 2 was used to extract maximum silica. To ensure maximum silica extraction from RHC, double extraction was performed on the residue of the first extraction and the final residue was tested for any remaining silica. The organic components of the residue were removed through combustion at 950 °C for 3 h. The resulting inorganic residue was subjected to dissolution in NaOH. The difference in the weight of residue before and after dissolution indicated whether any silica was not extracted by the first and double extraction.

It was found that the yield of extracted silica increased from 7.98 g with an SS:MeOH:H_2O ratio of 1:0.25:1 to a maximum of 9.84 g with an SS:MeOH:H_2O ratio of 1:0.10:1. The yield then remained constant at a value of approximately 9.2 g with SS:MeOH:H_2O ratio of 1:0.05:1 and 1:0:1. Considering the aforementioned results, the optimum ratio of SS:MeOH:H_2O was 1:0.10:1. The redissolution of the final inorganic residue in NaOH did not yield more than 0.5 g of silica in any case. Thus, more than 90% of the silica present in RHA could be obtained through double extraction, except when MeOH = 0.25 in the ratio SS:MeOH:H_2O. Thus, the extraction was economical. The average yield was 92.2%, which is highly suitable for industrial implementation. The experimental results are in good agreement with those from the literature [23].

3.3 FTIR, XRF, and BET-specific surface area analysis of silica particles

The silica samples obtained were irradiated using infrared radiations over a wavenumber range of 400–4000 cm^{-1} in a Shimadzu make FTIR. The radiations were transmitted through the sample to varying degrees depending on the bonds present in the sample and their motions. The transmission differences were obtained as peaks in the FTIR spectra of the samples. The results obtained are illustrated in Fig. 4. More than seven peaks were obtained for each silica sample.

Table 1 Comparison of kinetic parameters of RH and RS char in the present study with other researchers

Researchers	Biomass species	A (s^{-1})	E (kJ/mol)	σ (kJ/mol)	δ (%)
Gao et al. [42]	Rice husk	$0.024–6.118 \times 10^5$	120.97–235.68	–	–
Sattar et al. [43][a]	Rice husk	$1.9 \times 10^6–5.1 \times 10^9$	85.53–116.9	–	–
Sattar et al. [43][b]	Rice husk	$1.5 \times 10^8–1.4 \times 10^{13}$	111.87–151.39	–	–
Mansaray and Ghaly [44]	Rice husk	$1.18 \times 10^{14}–1.22 \times 10^{17}$	142.7–188.5	–	–
This study	Rice husk	$10^{8.7}$	128.13	5	0.066
	Rice straw	$10^{8.64}$	130.33	5	0.091

[a] Under N_2 atmosphere

[b] Under dry air atmosphere

Table 2 Extraction of silica from RHC with varying SS:MeOH:H_2O

Sr. No.	Weight of RHC produced from 50 g of RH (g)	Weight of RHA produced from 50 g of rice husk (g)	Weight of silica in 50 g of rice husk (g)[a] (A)	Extraction	SS:MeOH:H_2O	Weight of silica produced from extracted RHC (g) (B)	Yield of silica (%) (B/A) × 100
1.	21.0	10.5	9.975	First Re-extraction	1:0.25:1 1:0.25:1	6.92 1.06	80.0
				Total		7.98	
2.	21.0	10.5	9.975	First Re-extraction	1:0.20:1 1:0.20:1	8.88 0.34	92.43
				Total		9.22	
3.	21.0	10.5	9.975	First Re-extraction	1:0.15:1 1:0.15:1	9.0 0.68	97.04
				Total		9.68	
4.	21.0	10.5	9.975	First Re-extraction	1:0.10:1 1:0.10:1	9.22 0.62	98.65
				Total		9.84	
5.	21.0	10.5	9.975	First Re-extraction	1:0.05:1 1:0.05:1	8.42 0.78	92.23
				Total		9.2	
6.	21.0	10.5	9.975	First Re-extraction	1:0:1 1:0:1	7.06 2.2	92.83
				Total		9.26	

[a] RHA contains ~ 95% silica

Of these, the main peaks are the ones due to Si–O symmetric stretching of 797.05 and 800.42 cm^{-1} for samples 1 and 2, respectively, Si–OH asymmetric stretching of 3435.37 and 3435.21 cm^{-1} for samples 1 and 2, respectively, Si–O–Si asymmetric vibrations of 1049.08 and 1049.66 cm^{-1} for samples 1 and 2, respectively, and the –OH stretching vibration of silanol on the surface of silica of 1628.11 and 1633.76 cm^{-1} for samples 1 and 2, respectively. All peaks except that of the

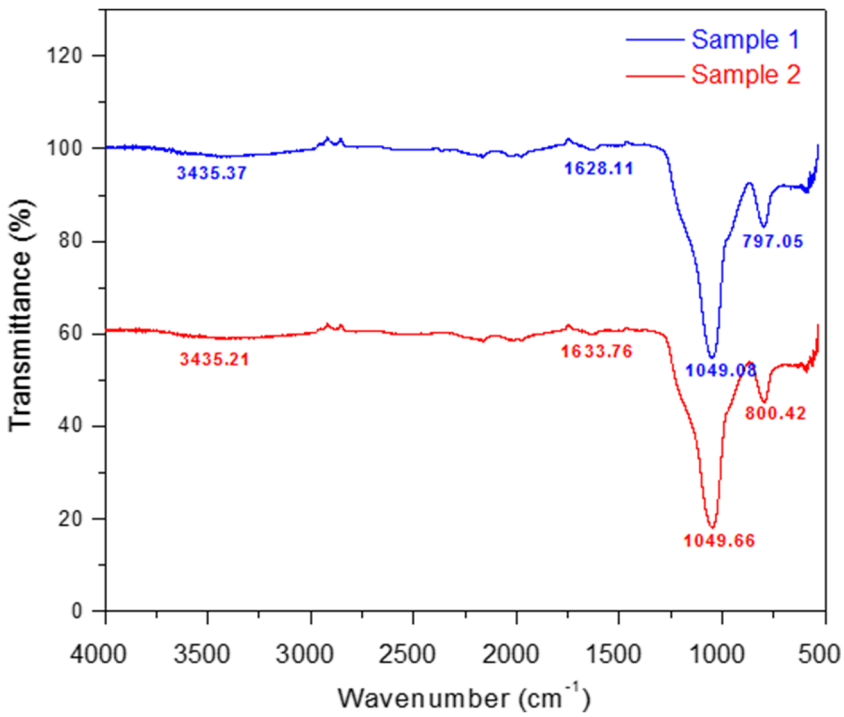

Fig. 4 FTIR spectrum of silica particles for different SS:MeOH:H_2O ratios: (1) SS:MeOH:H_2O = 1:0.15:1 and (2) SS:MeOH:H_2O = 1:0.10:1

Si–OH asymmetric bending vibration was obtained. Marginal differences were observed in the wavenumbers at which the peaks were obtained. The obtained wavenumbers were compared with the results from Zulkifli et al. [19]. They reported Si–O symmetric stretching of 802 cm^{-1}, Si–OH asymmetric stretching of 3450, Si–O–Si asymmetric vibrations of 1107 cm^{-1}, and the –OH stretching vibration of silanol of 1634 cm^{-1}. It was found that the results of samples 1 and 2 in Fig. 4 are in good agreement with Zulkifli et al. [19].

The purity of the samples was analyzed through Bruker model S8 Tiger and S4 Pioneer sequential wavelength-dispersive XRF analyzer. In the analysis, high-energy X-rays or gamma rays were bombarded on the surface of the sample. This bombardment caused the emission of secondary X-rays from the surface, which is characteristic to each compound. The obtained composition results are presented in Table 3. As presented in Table 3, the Si concentration of the RH sample was 97.35% and that of the RS sample was 98.26%. The impurities in the samples included Al_2O_3, Fe_2O_3, CaO, MgO, Na_2O, K_2O, and Cl and loss on ignition (LOI). The occurrence of these elements in the sample may be attributed to similar side reactions that may occur during the alkaline extraction of silica. The XRF study did not provide details regarding the form in which the aforementioned elements were present. However, the FTIR spectra indicated that Si was present as Si–O, Si–O–Si, and Si–OH bonds. Thus, the purity of the samples was above 97%, which is highly favorable for any application.

The specific surface area of the sample is a very important parameter because it determines the nature of interaction between the particles and base resin matrices, which are commonly used in composite preparations for different applications. The specific surface area is also an indirect indicator of the amorphous nature of the sample. Hence, the samples obtained were subjected to BET-specific surface area analysis in Smart make, BET analyzer. The BET analysis results are presented in Table 4. When varying the ratio of SS:MeOH:H_2O, the specific surface area varied in the range 298.85–381.8 m^2/g with an average specific surface area of 328 m^2/g which is highly favorable. The highest BET-specific surface area was obtained for an SS:MeOH:H_2O ratio of 1:0:1. The average specific surface area obtained in the present study is better than the specific surface area range of 150–200 m^2/g reported by Ghosh and Bhattacherjee [45] and 116–218 m^2/g reported by Bakar et al. [46].

Table 3 XRF elemental analysis of silica sample

Sr. No.	Elements (wt%)	RH	RS
1.	SiO_2	97.35	98.26
2.	Al_2O_3	0.13	0.19
3.	Fe_2O_3	0.02	0.02
4.	CaO	0.37	0.14
5.	MgO	0.27	0.12
6.	Na_2O	0.77	0.25
7.	K_2O	0.20	0.23
8.	Cl	0.09	0.09
9.	LOI	0.55	0.49
Total		99.79	99.75

3.4 FESEM analysis and imaging of silica particles

The obtained silica samples were imaged through FESEM using Nova Nano make FE-SEM 450 analyzer. Because the samples were nonconductive, they were sputter coated with gold and exposed to an emitted electron beam. The silica particle images obtained for SS:MeOH:H_2O ratios of 1:0.15:1 and 1:0.10:1 are illustrated in Fig. 5. The average particle size was estimated from the images and also different SS:MeOH:H_2O ratios of each sample are presented in Table 4. As indicated in Table 4, the size of silica particles decreased when the value of MeOH in the SS:MeOH:H_2O ratio decreased, with a minimum size of 40.32 nm for an SS:MeOH:H_2O of 1:0.05:1. The overall range of silica particle size was 22–170 nm. The particles were mostly spherical but agglomerated into clusters. These results are in good agreement with those from the literature [23]. The formation of clusters is highly unfavorable; hence, the direction of research was changed toward obtaining nanometer-sized monodispersed particles.

According to the assumption that the addition of water increases the dilution of the solution and enhances the formation of dispersed silica nanoparticles, the particle size and particle formation of a second set of samples were examined without adding methanol. The amount of water added to the solution was varied, and the silica yield was as presented in Table 5. The yield of silica is defined as the ratio of the weight of silica produced from extracted RHC to the weight of the silica in the RH. As in the previous cases, the maximum extraction of silica was ensured by conducting double extraction on the char residue and redissolving the inorganic residue after double extraction in NaOH. The difference in the weight of residue before and after dissolution indicated whether any silica was not extracted by the first and double extraction. This difference was always less than 0.5 g, which indicated that less than 5% of the total silica content in RHA was not extracted. In the aforementioned extractions, a consistent silica yield of 85.81–98.05% was obtained for 10.5 g of RHA.

The samples presented in Table 5 were analyzed using FESEM for identifying the particle formation and particle sizes. The samples were sputter coated with gold to make the surface conductive according to the principle of FESEM. The images obtained are displayed in Fig. S2. Varying the amount of water added during the silica extraction process did not support particle formation. Therefore, the assumption

Table 4 BET-specific surface area and average particle size of silica particles with varying methanol parts in SS:MeOH:H_2O ratio

Sr. No.	SS:MeOH:H_2O	Specific surface area (m^2/g)	Average D_P (nm)	Particle size range (nm)
1.	1:0.25:1	298.85	91.15	33.72–178.77
2.	1:0.20:1	342.27	89.47	29.87–171.0
3.	1:0.15:1	284.57	49.98	22–100.2
4.	1:0.10:1	336.53	43.70	35.55–62.51
5.	1:0.05:1	321.88	40.32	33.42–54.38
6.	1:0:1	381.80	41.71	14.66–69.73

that the dilution of SS by the addition of water before gelation has a major effect on the particle size of silica was rejected. The research was consequently directed toward finding a suitable size modifier by changing the alcohol. Only alcohols were considered despite the existence of other classes of alternatives, such as surfactants, because the interaction of these

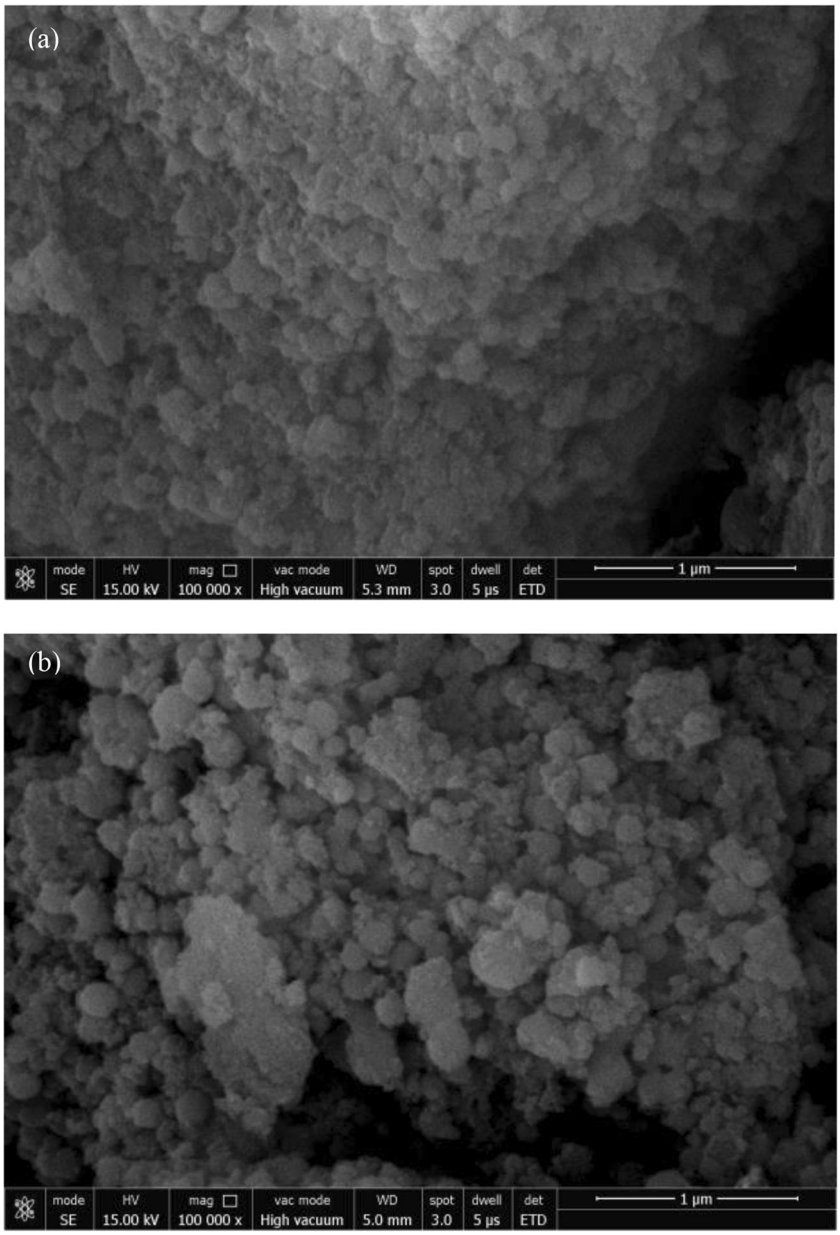

Fig. 5 FESEM images of silica particles for different SS:MeOH:H_2O ratios: **a** SS:MeOH:H_2O = 1:0.15:1 and **b** SS:MeOH:H_2O = 1:0.10:1

Table 5 Extraction of silica from RHC with varying SS:H_2O

Sr. No.	Weight of RHC produced from 50 g of RH (g)	Weight of RHA in 50 g of rice husk (g)	Weight of silica in 50 g of rice husk (g)[a] (A)	Extraction	SS:H_2O	Weight of silica produced from extracted RHC (g) (B)	Yield of silica (%) (B/A) × 100
1.	21.0	10.5	9.975	First	1:1.5	8.34	86.62
				Re-extraction	1:1.5	0.30	
				Total		8.64	
2.	21.0	10.5	9.975	First	1:1.25	8.86	90.23
				Re-extraction	1:1.25	0.14	
				Total		9.0	
3.	21.0	10.5	9.975	First	1:1	9.78	98.05
				Re-extraction	1:1	0.0	
				Total		9.78	
4.	21.0	10.5	9.975	First	1:0.75	8.46	88.42
				Re-extraction	1:075	0.36	
				Total		8.82	
5.	21.0	10.5	9.975	First	1:50	8.36	85.81
				Re-extraction	1:50	0.20	
				Total		8.56	

[a] RHA contains ~ 95% silica

alternative compounds differed considerably with the behavior of alcohols in the molecular environment of the SS solution. Therefore, MeOH, ethanol (EtOH), and *n*-propanol (PrOH) were selected for a comparative study.

The same procedure was used to conduct the silica extraction as in the previous experiments. Three size modifiers were considered to achieve particle formation as well as a small particle size. Silica extraction was performed by varying the amount of MeOH, EtOH, and PrOH before the gelation of the SS solution. The results obtained from the extraction are presented in Table 6. The SS:alcohol:H_2O of 1:0.10:1 is considered because as indicated in Table 2, the SS:MeOH:H_2O of 1:0.10:1 was given a maximum silica yield of 98.65%. Hence, other alcohols are compared with the same ratio. The yield remained constant as observed in the previous sample sets and ranged from 83.61 to 98.65%. The procedure described earlier in this section was used for obtaining the pure inorganic residue after silica extraction and for determining whether any silica was left to be extracted. Thus, the maximum yield of silica could be determined. After ensuring the highest possible yield of silica through double extraction, the extracted silica was again subjected to FESEM imaging to check for the formation of monodispersed silica nanoparticles. The results obtained are depicted in Fig. S3. Particle formation was not observed even after changing the size modifier from MeOH to EtOH and PrOH. An estimate of the particle size could be obtained from the observed particles; however, the nature and shape of the particles could not be confirmed. The results of particle size considering the same ratio of SS:alcohol:H_2O are also presented in Table 6. The particle size had an overall range of approximately 20.28–67.49 nm. However, particle formation could not be established because no spherical

Table 6 Extraction of silica from RHC with varying SS:alcohol:H_2O

Sr. No.	Weight of RHC produced from 50 g of RH (g)	Weight of RHA in 50 g of rice husk (g)	Weight of silica in 50 g of rice husk (g)[a] (A)	Extraction	SS:alcohol:H_2O	Weight of silica produced from extracted RHC (g) (B)	Yield of silica (%) (B/A) × 100	Average D_P (nm)	Particle size range (nm)
1.	21.0	10.5	9.975	First (MeOH)	1:0.10:1	9.22	98.65	43.70	35.55–62.51
				Re-extraction (MeOH)	1:0.10:1	0.62			
				Total		9.84			
2.	21.0	10.5	9.975	First (EtOH)	1:0.10:1	8.86	92.03	37.95	20.28–63.31
				Re-extraction (EtOH)	1:0.10:1	0.32			
				Total		9.18			
3.	21.0	10.5	9.975	First (PrOH)	1:0.10:1	8.20	83.61	43.02	20.73–67.49
				Re-extraction (PrOH)	1:0.10:1	0.14			
				Total		8.34			

[a] RHA contains ~ 95% silica

particles were visible in the images. The particles were lumped into micrometer-sized aggregates. These results are in good agreement with those from the literature [24].

3.5 Effect of the different agents and acid leaching on the purity of silica obtained from RH and RS

Silica was extracted from RH and RS using the methodology discussed in Fig. 2. Acid leaching was conducted at different stages to study its effect on the purity of the extracted silica. Moreover, the effect of the different agents on the purity of silica was studied by maintaining both nitrogen and air at a constant flow rate. The silica yield obtained is presented in Table 7. The silica content of RHA and RSA slightly vary from region to region. In general, the RHA contains ~ 95% silica while RSA contains ~ 72.8% silica. A higher volume of acid was required for leaching raw biomass than for leaching the pyrolyzed char and silica product. The yield of silica extracted from RH varied between 73.18 and 93.23%, whereas the yield of silica extracted from RS varied between 67.10 and 94.55%. In general, increased silica yield was observed when N_2 was used as the agent. The samples obtained when conducting acid leaching of the extracted silica reported a reduction in the weight by at least 0.6 g due to filtration losses which resulted in lower yields. To ensure that the product extracted was on par with the commercially available silica in the market, purity check was conducted on a sample of the extracted product. Because the original silica content of RH and RS was unknown, the samples of RH and RS ash were also prepared and subjected to an XRF test. In addition to the aforementioned two samples, the silica extracted from RH and RS samples at different stages of extraction by using different agents was also analyzed for purity through XRF analysis. The results of the XRF analysis and purity check are reported in Table 8.

As presented in Table 8, the silica samples from RH and RS that were acid leached after the extraction of silica exhibited a higher purity than the silica samples from acid-leached raw RH and RS samples and pyrolyzed char. When acid leaching was conducted on feed, the purity of silica was higher for RH samples than for RS samples. The purity of silica from the RH sample was 90.87 and 91.20%, and the purity of silica from the RS sample was 90.03 and 90.49% when using N_2 and air as the agent, respectively. When acid leaching was conducted on pyrolyzed char and extracted silica, the purity of silica was higher for RS samples than for RH samples. The purity of silica from the acid-leached char sample of RH was 84.91 and 89.06%, and the purity of silica from the acid-leached char sample of RS was 92.59 and 92.69% when using N_2 and air as the agent, respectively. The highest silica purity for the RS and RH samples was 98.26 and 97.35%, respectively, when acid leaching was conducted on the extracted silica by using N_2 as the agent. The silica purity of the RH and RS samples in the present study was 97.35 and 98.26%, respectively. These values are higher than the purity of commercial samples available in the market (95.52%). The high purity of the obtained silica enhances its favorability in the pharmaceutical, and food packaging sectors and for many industrial applications.

3.6 Economic analysis of production of silica of commercial-grade purity, activated char, and syngas from RH and RS in the process plant for Indian conditions

Figure 6 illustrates the percentages of char and syngas obtained from RH and RS at the optimum operating conditions in a two-stage pyrolysis and gasification process plant. The first stage of the reactor (Fig. 1) was operated at 600 °C, whereas

Table 7 Extraction of silica from RH and RS with different stages of acid leaching

Sample No.	Feed (50 g)	Weight of char produced from feed (g)	Weight of ash in 50 g of feed (g)	Weight of silica in feed (g)[a] (A)	Acid treatment	Volume of acid (ml)	Medium	Weight of silica extracted from RHC and RSC (g) (B)	Yield of silica (%) (B/A) × 100
1.	RH	21.0	10.5	9.975	Of RH	20	N_2	9.30	93.23
2.		21.0	10.5	9.975	Of RH	20	Air	8.06	80.80
3.		21.0	10.5	9.975	Of char	10	N_2	8.66	86.82
4.		21.0	10.5	9.975	Of char	10	Air	9.56	95.84
5.		21.0	10.5	9.975	Of extracted silica	6	N_2	7.30	73.18
6.		21.0	10.5	9.975	Of extracted silica	6	Air	7.94	79.60
7.	RS	18.5	6	4.368	Of RS	60	N_2	4.13	94.55
8.		18.5	6	4.368	Of RS	60	Air	3.68	84.25
9.		18.5	6	4.368	Of char	40	N_2	3.69	84.48
10.		18.5	6	4.368	Of char	40	Air	3.21	73.49
11.		18.5	6	4.368	Of extracted silica	6	N_2	3.48	79.67
12.		18.5	6	4.368	Of extracted silica	6	Air	2.93	67.10

[a] RHA contains ~ 95% silica while RSA contains ~ 72.8% silica

Table 8 XRF report of silica samples from RH and RS with different agents and different stages of acid leaching

Sample/ element	Feed	Substrate of acid treatment	Agent	SiO_2	Al_2O_3	Fe_2O_3	CaO	MgO	Na_2O	K_2O	SO_3	Cl	LOI
Commercial[a]	–	–	–	95.52	0.30	0.06	0.04	1.06	1.55	ND	1.12	0.05	0.23
RHA	RH	–	–	95.01	0.13	0.15	0.71	0.39	0.07	0.36	0.41	0.52	2.77
RSA	RS	–	–	72.80	0.65	0.47	3.68	3.25	3.15	10.73	2.15	0.72	0.01
Sample 1	RH	RH	N_2	90.87	0.09	0.02	0.38	0.18	4.00	0.03	0.07	3.87	0.47
Sample 2	RH	RH	Air	91.20	0.08	0.02	0.23	0.12	3.75	0.06	0.08	3.96	0.39
Sample 3	RH	char	N_2	84.91	0.09	0.03	0.25	0.14	6.77	0.07	0.09	7.14	0.42
Sample 4	RH	char	Air	89.06	0.12	0.02	0.24	0.10	4.80	0.05	0.07	5.13	0.38
Sample 5	RH	Extracted silica	N_2	97.35	0.13	0.02	0.37	0.27	0.77	0. 20	ND	0.09	0.55
Sample 7	RS	RS	N_2	90.03	0.22	0.02	0.26	0.22	4.25	0.13	0.07	4.13	0.50
Sample 8	RS	RS	Air	90.49	0.24	0.05	0.30	0.27	3.72	0.07	0.07	4.04	0.44
Sample 9	RS	char	N_2	92.59	0.34	0.05	0.41	0.22	2.99	0.20	0.09	2.66	0.43
Sample 10	RS	char	Air	92.69	0.33	0.03	0.33	0.23	3.09	0.06	0.09	2.65	0.48
Sample 11	RS	Extracted silica	N_2	98.26	0.19	0.02	0.14	0.12	0.25	0.23	0.02	ND	0.49

[a] Commercial sample used for comparison

the second stage of the reactor was operated at 875 °C. The amounts of char, tar, and gas produced at this optimum condition were 40.5, 6.85, and 52.65 wt% for RH, respectively, and 37.05, 7.75, and 55.2 wt% for RS, respectively. Because RH and RS contained 21 and 12 wt% RHA and RSA, respectively, the net amount of char produced from RH and RS was

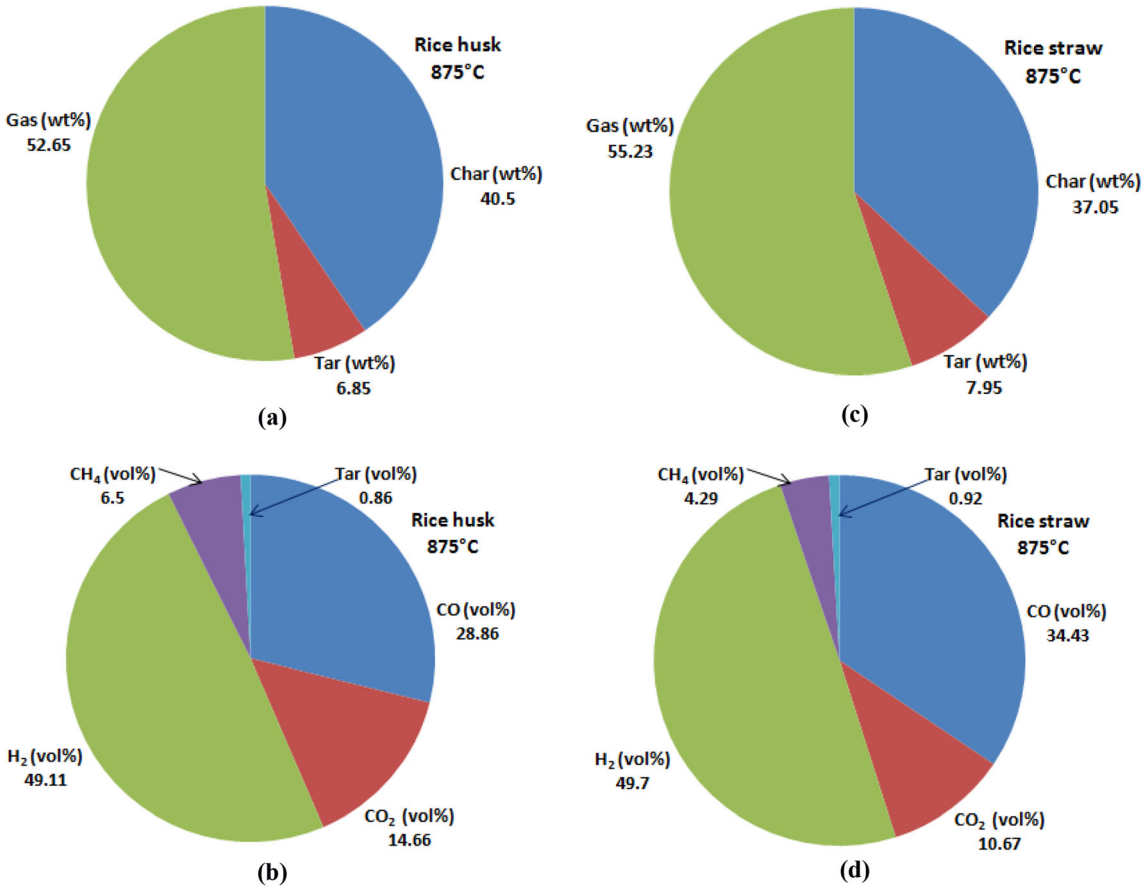

Fig. 6 Comparison of yield obtained from RH and RS at the optimum temperature **a** char, tar, and syngas from RH, **b** individual component gases from RH, **c** char, tar, and syngas from RS, and **d** individual component gases from RS

Table 9 Cost of production and revenue generated from RH/RS processing plant considering the market price of commercial-grade silica equal to US$26.395/kg

Sr. No.	Particulars	Cost in USD per kg of commercial-grade silica produced
Basis: 1 MT/day of RH (plant cost ~ US$0.1 million)		
1.	Raw material	0.263 (at US$0.039/kg)
2.	Consumables	0.033
3.	Cost of manpower	0.033
4.	Maintenance cost	0.026
5.	Power cost per kWh	0.066 (generated in house)
6.	Packing, handling, and transportation	0.066
7.	Thermal energy	0.079 (residual heat generated in house)
8.	Depreciation on plant and machinery, building, office equipment, etc. (10 years)	0.066
9.	Interest at 15%	0.079
10.	Total cost of production	0.711
11.	Total cost of production for 180 kg of silica	US$127.98
12.	Revenue generated	
	• Cost of 180 kg of silica produced	US$4751.1/kg
	• Cost of 175 kg of activated carbon (at US$0.329/kg)	US$57.575
	• Cost of 0.5 MWh of electricity produced (at US$0.066/kWh)	US$33.0
	• Cost of 0.5 MWh of thermal energy produced (at US$0.079/kWh)	US$39.5
	• Total	US$4881.175
13.	Net profit	US$4753.0
Basis: 1 MT/day of RS (plant cost ~ US$0.1 million)		
1.	Raw material	0.263 (at US$0.039/kg)
2.	Consumables	0.033
3.	Cost of manpower	0.033
4.	Maintenance cost	0.026
5.	Power cost per kWh	0.066 (generated in house)
6.	Packing, handling, and transportation	0.066
7.	Thermal energy	0.079 (residual heat generated in house)
8.	Depreciation on plant and machinery, building, office equipment, etc (10 years)	0.066
9.	Interest at 15%	0.079
10.	Total cost of production	0.711
11.	Total cost of production for 85 kg of silica	US$60.435
12.	Revenue generated	
	• Cost of 85 kg of silica produced (at US$26.395/kg)	US$2243.575
	• Cost of 250 kg of activated carbon (at US$0.329/kg)	US$82.25
	• Cost of 0.5 MWh of electricity produced (at US$0.066/kWh)	US$33.0
	• Cost of 0.5 MWh of thermal energy produced (at US$0.079/kWh)	US$39.5
	• Total	US$2398.325
13.	Net profit	US$2337.0

19.5 and 25.05 wt%, respectively. The maximum amount of clean syngas (CO + H_2) was 84.58 vol% for RS and 77.97 vol% for RH. The gas compositions were analyzed using Shimadzu make gas chromatograph. The aforementioned optimum product compositions were used to analyze the plant economics of production of silica of commercial-grade purity, activated char, and syngas from RH and RS as per the Indian condition. The cost of production includes raw material, consumables, manpower cost, power cost, thermal energy cost, packing, handling and transportation cost,

depreciation, and interest [47]. The total cost of production was calculated according to the amount of silica produced in kilograms. The electrical and thermal efficiencies of the plant were considered 37 and 49%, respectively, to produce 0.5 MWh of electricity and 0.5 MWh of thermal energy from 1 ton of RH or RS [48, 49]. The total fixed capital cost of setting up plant to process 1 MT/day of RH or RS includes the details of the needed equipment cost, land and building cost, and other fixed asset cost as given in Table S2. It would be approximately US$0.1 million as per the Indian condition. The revenue generated from the production of silica of commercial-grade purity, activated carbon, electricity, thermal energy, and possible net profit from this plant is reported in Table 9 and Table S1. Table 9 considers the market price of commercial-grade silica equal to US$26.395/kg, while Table S1 considers the price of silica equal to US$0.95/kg as reported in the literature [47]. The net profit for a RH and RS processing plant is US$173.0 and 175.0, respectively, as presented in Table S1 while the net profit for a RH and RS plant skyrockets to US$4753.0 and 2337.0, respectively, as presented in Table 9. As presented in Table 8, commercial-grade silica currently available in the market at US$26.395/kg with a purity of 95.52% is less than the commercial-grade silica obtained from RH and RS in the present study with a purity of 97.35 and 98.26%, respectively.

4 Conclusions

Silica is obtained through the pyrolysis of RH or RS followed by the alkaline extraction of pyrolyzed char. The Gaussian distribution of the activation energy model had a superfit with the experimental data of RH and RS char. The production of silica can be structurally controlled by the addition of size-control agents. Alcohols were used in this study to vary the size of silica particles. The size of the produced silica particles reduced when reducing the amount of methanol added (i.e., when reducing the value of MeOH in the ratio SS:MeOH:H_2O). The particle diameter varied over a broad range of 22–170 nm, and the particles were spherical but agglomerated. The extraction of silica was economical, with an average yield of 92.2%. FTIR analysis confirmed the presence of Si–O–Si, Si–O, and Si–OH bonds in the samples. The specific surface area of the samples was very high, with an average value of 328 m^2/g. To find a suitable size-control agent, three alcohols were used, namely methanol, ethanol, and propanol. The obtained silica particles were similar in nature and lumped as micro-sized particles. Thus, additional research is required regarding aspects such as the temperature of gelation, controlling the rate of gelation, and alternative procedures for silica extraction. The results indicated that the silica samples obtained from RS were purer than those obtained from RH. Moreover, the results indicated that nitrogen is a better agent than air and that acid leaching must be performed on the extracted silica rather than on the feed and pyrolyzed char to obtain higher purity silica. The purity of commercial-grade silica obtained from RH and RS in the present study was 97.35 and 98.26%, respectively. These values were higher than the purity of the commercial silica used in this study (95.52%). Therefore, the silica produced in the present study can be considered suitable for various applications in areas such as the food and nutrition sector and pharmaceutical industry as well as for being used as a potential nanosized catalyst.

Acknowledgments The authors wish to acknowledge the contribution of Visvesvaraya National Institute of Technology, Nagpur, India for providing experimental and other necessary facilities to carry out this research work.

References

1. Ministry of Agriculture and Farmers Welfare, India (2018) Report No. Krishi-AR-2017-18-1
2. Nakhshiniev B, Biddinika MK, Gonzales HB, Sumida H, Yoshikawa K (2014) Evaluation of hydrothermal treatment in enhancing rice straw compost stability and maturity. Bioresour Technol 151:306–313
3. Kurama S, Kurama H (2008) The reaction kinetics of rice husk based cordierite ceramics. Ceram Int 34:269–272
4. Awizar DA, Othman NK, Jalar A, Daud AR, Rahman IA, Al-Hardan NH (2013) Nanosilicate extraction from rice husk ash as green corrosion inhibitor. Int J Electrochem Sci 8:1759–1769
5. Janowska G, Rybinski P, Jantas R (2007) Effect of themodification of silica on thermal properties and flammability of cross-linked butadiene–acrylonitrile rubbers. J Therm Anal Cal 87:511–517
6. Uribe NC, Echeverry CA, Velez MB, Jaramillo L, Martinez J (2018) Possibilities of rice husk ash to be used as reinforcing filler in polymer sector-a review. Revista UIS Ingenierias 17:127–142
7. Shen Y (2017) Rice husk silica derived nanomaterials for sustainable applications. Renew Sustain Energy Rev 80:453–466
8. Khaleghian H, Molaverdi M, Karimi K (2017) Silica removal from rice straw to improve its hydrolysis and ethanol production. Ind Eng Chem Res 56:9793–9798
9. Rajamani D, Surender R, Mahendran A, Muthusubramanian S, Vijayakumar C (2013) Bismaleimide/rice husk silica reinforced composites. J Therm Anal Cal 114:883–893
10. Adam F, Appaturi JN, Khanam Z, Thankappan R, Nawi MAM (2013) Utilization of tin and titanium incorporated rice husk silica nanocomposite as photocatalyst and adsorbent for the removal of methylene blue in aqueous medium. Appl Surf Sci 264:718–726
11. Salavati-Niasari M, Javidi J, Dadkhah M (2013) Ball milling synthesis of silica nanoparticle from rice husk ash for drug delivery application. Comb Chem High Throughput Screening 16:458–462
12. Bajpai PK, Rao MS, Gokhale KVGK (1981) Synthesis of mordenite type zeolite using silica from rice husk ash. Ind Eng Chem Prod Res Dev 20:721–726
13. Ghodke P, Mandapati RN (2018) Kinetic modeling of Indian rice husk pyrolysis. Int J Chem React Eng 16:1–15
14. Selvakumar KV, Umesh A, Ezhilkumar P, Gayatri S, Vinith P, Vignesh V (2014) Extraction of silica from burnt paddy husk. Int J ChemTech Res 6:4455–4459

15. Ang TN, Ngoh GC, Chua ASM (2013) Comparative study of various pretreatment reagents on rice husk and structural changes assessment of the optimized pretreated rice husk. Bioresour Technol 135:116–119
16. Yalcin N, Sevinc V (2001) Studies on silica obtained from rice husk. Ceram Int 27:219–224
17. Patel M, Karera A, Prasanna P (1987) Effect of thermal and chemical treatments on carbon and silica contents in rice husk. J Mater Sci 22:2457–2264
18. Javed SH, Naveed S, Ramzan N, Feroze N, Zafar M (2010) Characterization of amorphous silica obtained from KMnO4 treated rice husk. J Chem Soc Pak 32:78–82
19. Zulkifli NSC, Rahman IA, Mohamad D, Husein A (2013) A green sol-gel route for the synthesis of structurally controlled silica particles from rice husk for dental composite filler. Ceram Int 39:4559–4567
20. Iler RK (1979) Silica gels and powders. In: Iler RK (ed) The chemistry of silica. Wiley, New York, pp 462–599
21. Kamath SR, Proctor A (1998) Silica gel from rice hull ash: preparation and characterization. Cereal Chem 75:484–487
22. Fujita K, Ikemi T, Nishiyama N (2011) Effects of particle size of silica filler on polymerization conversion in a light-curing resin composite. Dent Mater 27:1079–1085
23. Kim J, Kim L, Kim C (2007) Size control of silica nanoparticles and their surface. Biomacromol 8:215–222
24. Yun DS, Kim HJ, Yoo JW (2005) Preparation of silica nanospheres: effect of silicon alkoxide and alcohol on silica nanospheres. Bull Korean Chem Soc 26:1927–1928
25. Khonde R, Chaurasia A (2016) Rice husk gasification in a two-stage fixed-bed gasifier: production of hydrogen rich syngas and kinetics. Int J Hydrogen Energy 41:8793–8802
26. Kate GU, Chaurasia AS (2018) Gasification of rice husk in two-stage gasifier to produce syngas, silica and activated carbon. Energy Sources Part A 40:466–471
27. Krishnarao RV, Subrahmanyam J, Kumar J (2001) Studies on the formation of black particles in rice husk silica ash. J Eur Ceram Soc 21:99–104
28. Liou TH (2004) Preparation and characterization of nano-structured silica from rice husk. Mater Sci Eng A 364:313–323
29. Shen J, Liu X, Zhu S, Zhang H, Tan J (2011) Effects of calcinations parameters on the silica phase of original and leached rice husk ash. Mater Lett 65:1179–1183
30. Zeng X, Wang Y, Yu J, Wu S, Zhong M, Xu S, Xu G (2011) Coal pyrolysis in a fluidized bed for adapting to a two-stage gasification process. Energ Fuel 25:1092–1098
31. Gautam N, Chaurasia A (2020) Study on kinetics and bio-oil production from rice husk, rice straw, bamboo, sugarcane bagasse and neem bark in a fixed-bed pyrolysis process. Energy 190:1–13
32. Khonde RD, Nanda J, Chaurasia AS (2018) Experimental investigation of catalytic cracking of rice husk tar for hydrogen production. J Mater Cycles Waste Manage 20:1310–1319
33. Khonde RD, Chaurasia AS (2017) Tar cracking of rice husk in biomass gasifier: Reactor design and experimentation. Indian J Chem Technol 24:55–60
34. A Nunes SM, Paterson N, Herod AA, Dugwell DR, Kandiyoti R (2008) Tar formation and destruction in a fixed bed reactor simulating downdraft gasification: optimization of conditions. Energ Fuel 22:1955–1964.
35. Chen Y, Luo YH, Wu WG, Su Y (2009) Experimental investigation on tar formation and destruction in a lab-scale two-stage reactor. Energ Fuel 23:4659–4667
36. Dabai F, Paterson N, Millan M, Fennel P, Kandiyoti R (2010) Tar formation and destruction in a fixed-bed reactor simulating downdraft gasification: equipment development and characterization of tar-cracking products. Energ Fuel 24:4560–4570
37. Kandiyoti R, Herod A, Bartle K (2006) Solid fuels and heavy hydrocarbon liquids: thermal characterization and analysis. Elsevier, London
38. Ahrenfeldt J, Henriksen U, Jensen TK, Gøbel B, Wiese L, Kather A, Egsgaard H (2006) Validation of a continuous combined heat and power (CHP) operation of a two-stage biomass gasifiers. Energ Fuel 20:2672–2680
39. Chaurasia A (2016) Modeling of downdraft gasifier: studies on chemical kinetics and operating conditions on the performance of the biomass gasification process. Energy 116:1065–1076
40. Chaurasia A (2018) Modeling of downdraft gasification process: studies on particle geometries in thermally thick regime. Energy 142:991–1009
41. Chaurasia A (2019) Modeling of downdraft gasification process: part I—studies on shrinkage effect on tabular, cylindrical and spherical geometries. Energy 169:130–141
42. Gao X, Zhang Y, Xu F, Yin Z, Wang Y, Bao F, Li B (2019) Experimental and kinetic studies on the intrinsic reactivities of rice husk char. Renewable Energy 135:608–616
43. Sattar H, Muzaffar I, Munir S (2020) Thermal and kinetic study of rice husk, corn cobs, peanut crust and Khushab coal under inert (N_2) and oxidative (dry air) atmospheres. Renewable Energy 149:794–805
44. Mansaray KG, Ghaly AE (1999) Determination of kinetic parameters of rice husks in oxygen using thermogravimetric analysis. Biomass Bioenergy 17:19–31
45. Ghosh R, Bhattacherjee S (2013) A review study on precipitated silica and activated carbon from rice husk. J Chem Eng Process Technol 4:1–7
46. Bakar RA, Yahya R, Gan SN (2016) Production of high purity amorphous silica from rice husk. Procedia Chem 19:189–195
47. Subbukrishna DN, Suresh KC, Paul PJ, Dasappa S, Rajan NKS (2007) Precipitated silica from rice husk ash by IPSIT process. 15th European Biomass Conference & Exhibition, Berlin, Germany, pp. 2091–2093
48. Kumar A, Demirel Y, Jones DD, Hanna MA (2010) Optimization and economic evaluation of industrial gas production and combined heat and power generation from gasification of corn stover and distillers grains. Bioresour Technol 101:3696–3701
49. Lehmann J (2007) Bio-energy in the black. Front Ecol Environ 5: 381–387